

Fluorescence Determination of Warfarin Using TGA-capped CdTe Quantum Dots in Human Plasma Samples

A. Dehbozorgi¹ · J. Tashkhourian¹ · S. Zare¹

Received: 4 July 2015 / Accepted: 28 September 2015 / Published online: 19 October 2015
© Springer Science+Business Media New York 2015

Abstract In this study, some effort has been performed to provide low temperature, less time consuming and facile routes for the synthesis of CdTe quantum dots using ultrasound and water soluble capping agent thioglycolic acid. TGA-capped CdTe quantum dots were characterized through x-ray diffraction, transmission electron microscopy, Fourier transform infrared, ultraviolet-visible and fluorescence spectroscopy. The prepared quantum dots were used for warfarin determination based on the quenching of the fluorescence intensity in aqueous solution. Under the optimized conditions, the linear range of quantum dots fluorescence intensity versus the concentration of warfarin was 0.1–160.0 μM , with the correlation coefficient of 0.9996 and a limit of detection of 77.5 nM. There was no interference to coexisting foreign substances. The selectivity of the sensor was also tested and the results show that the developed method possesses a high selectivity for warfarin.

Keywords Quantum dots · CdTe QDs · Warfarin · Fluorescence

Introduction

Quantum dots (QDs) are semiconductor nanoparticles with particular optical and electronic properties that have been widely studied and applied in the last decade [1–4]. Some of

the most attractive properties of QDs are broad absorption spectra, high molar extinction coefficients, high quantum yield, narrow and symmetric emission bands, large effective Stokes shifts and high resistance to photobleaching and chemical degradation [5]. Quantum dots are very versatile labels because their photoluminescence emission band can be easily tuneable, from the UV to the IR regions, by the selection of the particle size (1–12 nm) and the nature and composition of the nanoparticle. Due to their excellent photophysical, magnetic, electronic and biological properties, quantum dots are widely applied in medical field for bio tracking of drug molecules [6, 7], bioimaging [8, 9], biosensing [10, 11], disease detection [12], photodynamic therapy [13], antimicrobial prevention [14] and molecular biology [15]. An interesting review describing recent developments of the QD application in nanomedicine was recently published by Wang and Chen [16].

The conventional methods for preparing quantum dots suffer from several limitations, such as high processing temperature, relatively high cost, nonstoichiometric compositions, and poor crystallinity. Recently, the ultrasonic and microwave irradiation have found widespread use in the aqueous synthesis (Ultrasonic-/Microwave-assisted synthesis) of different nanomaterials especially for quantum dots [17–19]. This is due to their simplicity, narrower size distribution, good shape control of nanomaterials, lower temperature for synthesis, better control of surface and their higher synthesis rate [20, 21].

A typical sonochemical preparation of these materials involves the ultrasonic irradiation of an aqueous solution of a metal salt and a chalcogen (e.g., S, Se and Te) source in which the in-situ-generated H_2S or H_2Se by sonication reacts with sonochemically decomposed metal salts to produce metal chalcogenide nanoparticles [22]. Using a structure directing agent, a variety of nanostructures such as nanorods, nanowires, or nanocubes can be prepared [23–26].

✉ J. Tashkhourian
tashkhourian@susc.ac.ir

¹ Department of Chemistry, College of Sciences, Shiraz University, Shiraz 71456, Iran

Warfarin 3-(α -acetylbenzyl)-4-hydroxycoumarin (WAR) (Fig. 1) is widely used as an oral anticoagulant and functions as a vitamin K antagonist by inhibiting the synthesis of vitamin K reductase and vitamin K epoxide reductase, thus decreasing the ability of blood to form clot. The concentration of WAR in plasma must be carefully monitored by repeated analysis of prothrombin time (international normalized ratio, INR) because WAR has a very narrow therapeutic window which leads to a very large variation in dosage required for optimal INR. Furthermore, (R)- and (S)-enantiomers of WAR exhibit considerable differences in pharmacokinetic and pharmacodynamic properties [27]. Historically, high performance liquid chromatography (HPLC) with UV detection is commonly seen as the analytical method for the determination of warfarin enantiomers [28–30] and also micellar electrokinetic chromatography–mass spectrometry (MEKC–MS) [31] was reported.

In this study, TGA-capped CdTe QDs has been used for selective determination of warfarin by fluorometric method. Thioglycolic acid capped CdTe quantum dots were synthesized through a sonochemical method. The effects of several important factors were investigated to find optimum conditions. Finally the method was used for the determination of warfarin in human blood plasma.

Experimental

Materials and Reagents

Cadmium nitrate tetrahydrate ($\text{Cd}(\text{NO}_3)_2 \cdot 4\text{H}_2\text{O}$), sodium borohydride (NaBH_4), thioglycolic acid (TGA), sodium hydroxide (NaOH), potassium nitrate (KNO_3), ethanol, acetone, boric acid (H_3BO_3), acetic acid, sodium carbonate (Na_2CO_3), Tris-hydroxymethyl-methane (Tris), phosphoric acid (H_3PO_4), ammonia (NH_3), sodium chloride (NaCl), hydrochloric acid (HCl), phenol, dichlorophenol and citric acid (CA) were purchased from Merck Chemical company. Ascorbic acid (AA), naproxen, folic acid, aspirin,

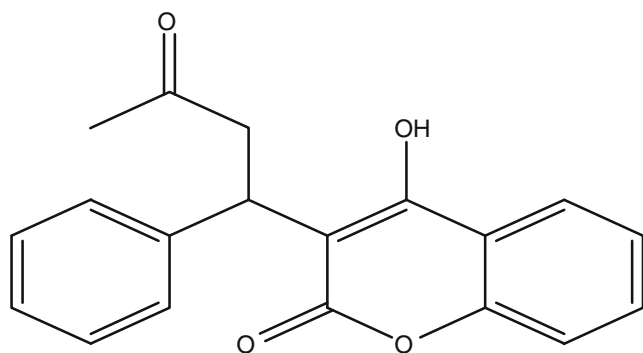


Fig. 1 Molecular structure of warfarin

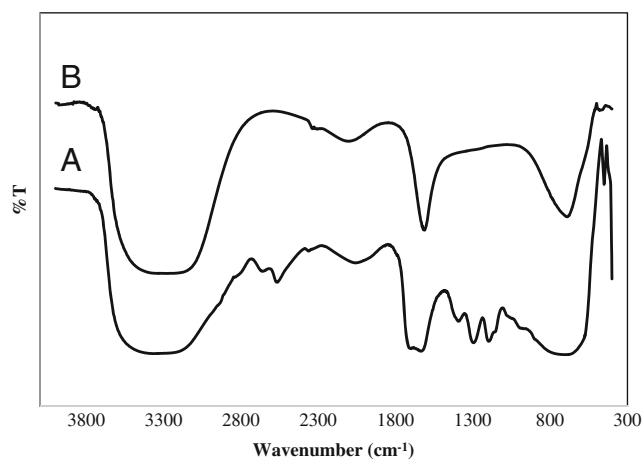


Fig. 2 ATR spectra of **a** TGA and **b** TGA-CdTe QDs

acetaminophen and ibuprofen were obtained from Fluka. Tellurium powder (Te), amoxicillin, ampicillin and warfarin were purchased from Sigma Aldrich. All reagents were of analytical grade and used as supplied without further purification.

Phosphate buffer solutions (PBS) were prepared by the addition of appropriate amounts of concentrated NaOH to 0.01 mol L^{-1} phosphoric acid solutions. Tris-saline buffers were prepared by the addition of appropriate amounts of concentrated HCl to the solution containing the 0.05 mol L^{-1} Tris- HCl and 0.10 mol L^{-1} NaCl to obtain different pH values. The universal Britton-Robinson buffer solutions over required pH values were prepared by addition of appropriate amount of 0.20 mol L^{-1} NaOH to a solution of mixed acid, being 0.04 mol L^{-1} with respect to phosphoric acid, acetic acid and boric acid.

Apparatus

All fluorescence spectra were recorded on a Perkin-Elmer LS50B Spectrofluorometer equipped with a thermostated cell compartment containing quartz cuvettes (1.0 cm). UV-Vis

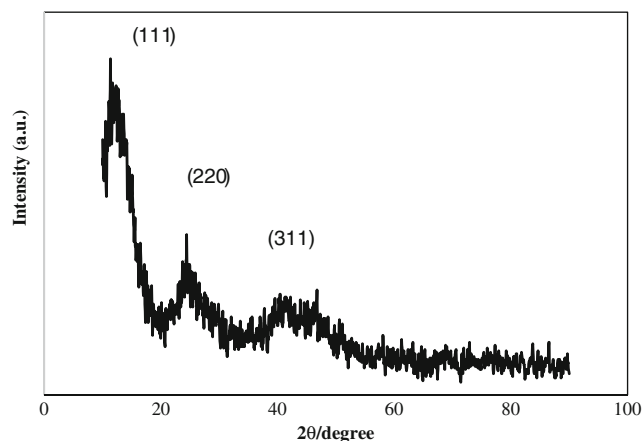


Fig. 3 XRD patterns of TGA-CdTe QDs

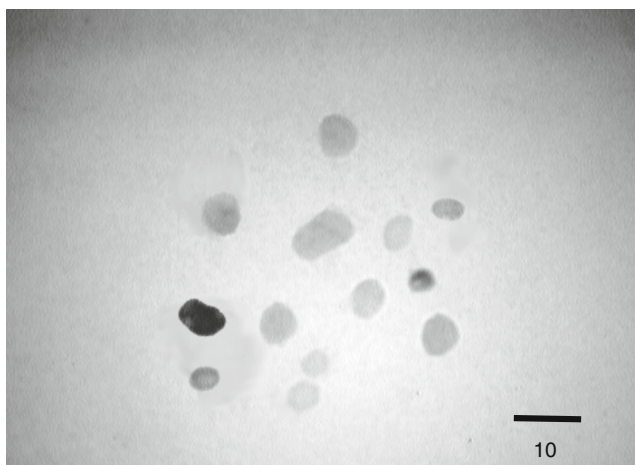


Fig. 4 TEM photograph of TGA-CdTe QDs

spectra were recorded using Unico 4802 UV-Vis double beam spectrophotometer employing quartz or glass cuvette with 1.0 cm path length. Hielscher ultrasonic processor probe (model UP200H) was used for synthesis of quantum dots and a SIGMA (model 2-6E) centrifuge was used for centrifugating. Different methods were applied for characterization of the synthesized quantum dots, including FT-IR spectroscopy (FTIR-8300 Shimadzu), attenuated total reflection (ATR) spectroscopy using Perkin-Elmer FT-IR spectrophotometer (model Spectrum RX I), XRD (Bruker D8 Advance with Cu-K α , $\lambda=0.1542$ nm) and transmission electron microscopy (TEM, Zeiss – EM10C – 80 KV). The pH measurements were made with a Metrohm 708 pH meter using a combined glass electrode.

Ultrasound-Assisted Synthesis of TGA-capped CdTe Quantum Dots [32]

First, 10.0 mL of deionized water was added to the tellurium powder (0.1 mmol) and then sodium borohydride (0.4 mmol)

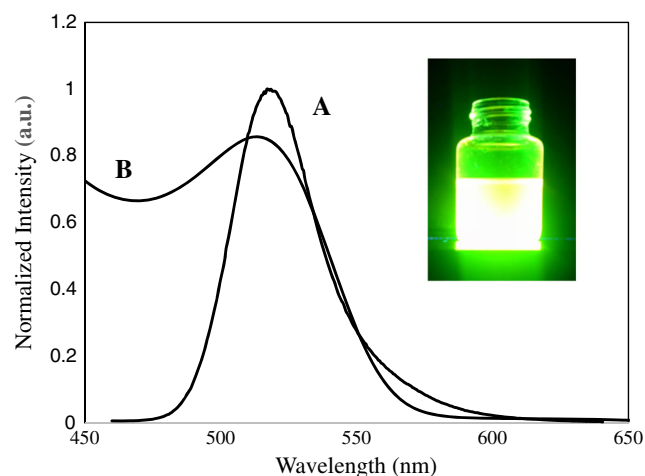


Fig. 5 FL(a) and UV-Vis spectra(b) of TGA-CdTe QDs solution. Inset: Fluorescence of TGA-CdTe QDs under UV irradiation (366 nm)

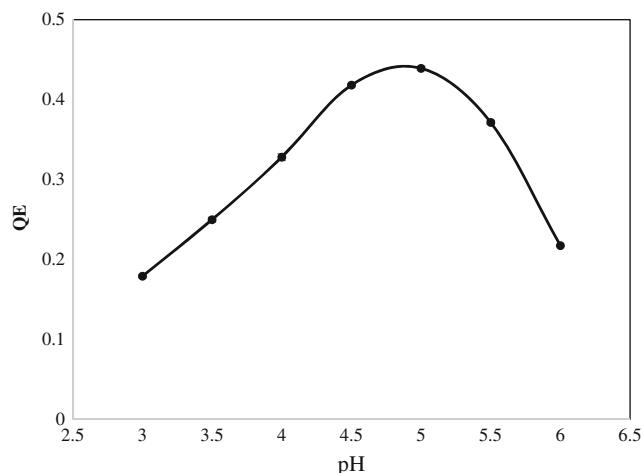


Fig. 6 Effect of pH on the quenching of TGA-CdTe QDs with 10.0 μM of warfarin

was added to the tellurium dispersion, and this second mixture was irradiated with 100 % ultrasonic power (200.0 W) until reduction of all Te. Finally, a clear, colorless solution was obtained. The entire reduction process was conducted in degassed deionized water (with N₂ for 10.0 min).

While the sonication power is 100 %, 5.0 mL of the reduced solution was rapidly injected into a Cd(NO₃)₂·4H₂O (20.0 mL 1.0×10⁻⁴ mol L⁻¹) alkaline solution pH, containing capping agent (TGA) while still sonicating (100 % power). While sonication the fluorescence of the solution was appeared and could be tuned by controlling the sonication time. Then, the solution is cooled down to room temperature and mixed with ethanol and subjected to centrifugation at 4000 rpm for 5.0 min in order to separate the QDs by precipitation. After centrifugation, the supernatant liquid phase was decanted to remove any excess reagents. Afterwards, the precipitate was washed three times with 25.0 mL ethanol and then dispersed in water. This solution can be kept for several

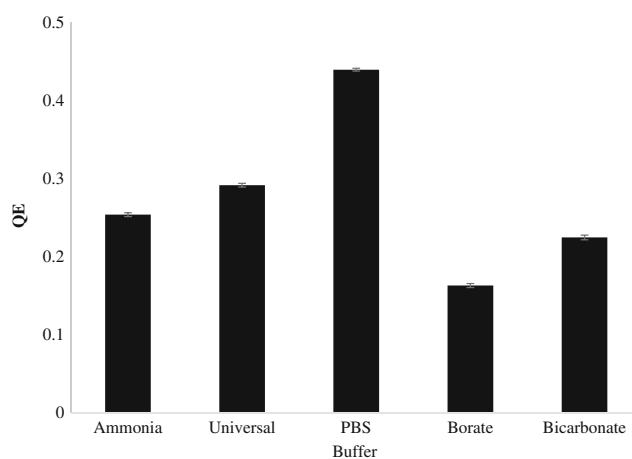


Fig. 7 Quenching efficiency for addition of 10.0 μM warfarin to TGA-CdTe QDs in different buffers

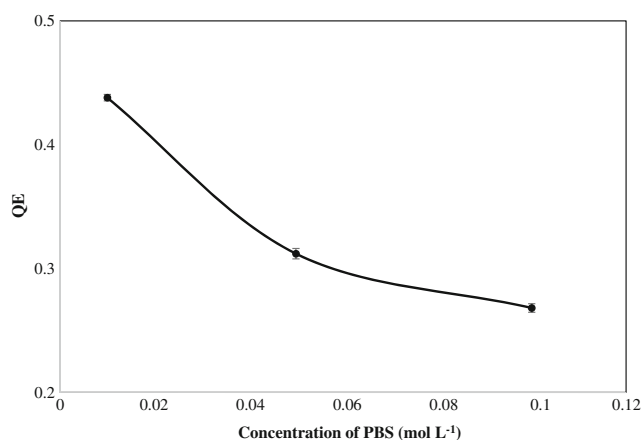


Fig. 8 Effect of buffer concentration on QD's quenching in the presence of 10.0 μM warfarin

months without any obvious aggregation and change in fluorescence spectra.

Procedure

All experiments were performed with excitation wavelength of 395 nm, emission range of 470–650 nm in pH 5.5 phosphate buffer solution (PBS). Excitation and emission slits were fixed at 5.0 nm width. For each experiment, 60.0 μL of QDs stock solution, 3.5 mL of buffer and appropriate amount of warfarin stock solution were added to a 5.0 mL volumetric flask, diluted to the mark and subjected to stirring. The fluorescence spectra were recorded in different time intervals to optimize the incubation time. The study of possible interferences was performed for binary mixtures of warfarin (10.0 μM) and the interfering material.

Fig. 9 Effect of ionic strength on the quenching of TGA-CdTe QDs in the presence of 10.0 μM warfarin. *Inset plot* shows the effect of ionic strength by means of QE

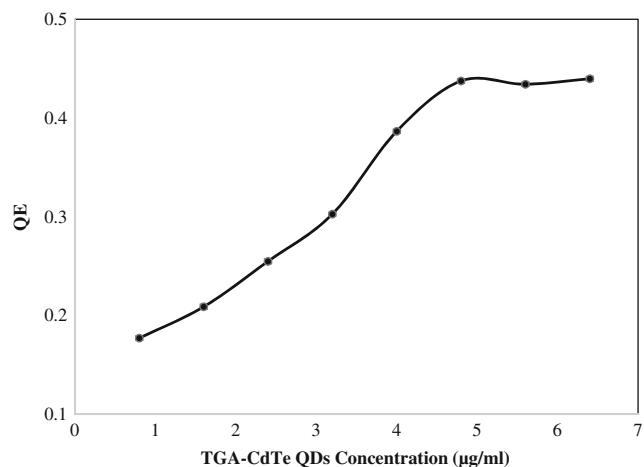
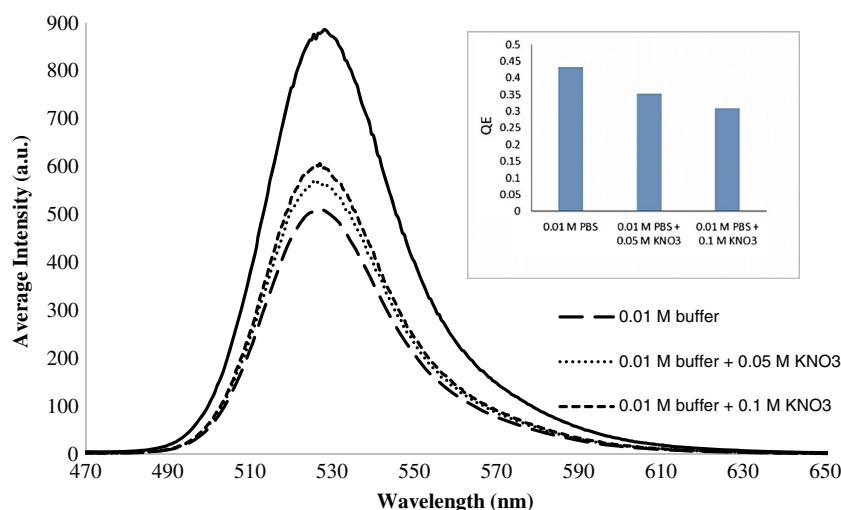


Fig. 10 Effect of QDs concentration on the quenching efficiency in the presence of 10.0 μM warfarin

Results and Discussion

CdTe QDs were synthesized and stabilized by using water soluble thioglycolic acid. In addition to serving as stabilizer, thioglycolic acid serves to: (i) passivate the surface of QDs and thereby removing the surface traps which lower the photoluminescence efficiency of the quantum dots, (ii) prevent the non-radiative recombination of electron and hole and (iii) control growth kinetics thereby prevent aggregation via steric hindrance [33, 34]. The capping agent is also a means by which QDs interact with other molecules and their environment through covalent attachments, electrostatic forces and hydrogen bonding [35, 36].

Structural Properties of TGA-capped CdTe QDs

The first characterization performed for TGA-CdTe QDs was attenuated total reflection/Fourier transform infrared (ATR/FTIR). Figure 2 shows the ATR/FTIR spectra for TGA and

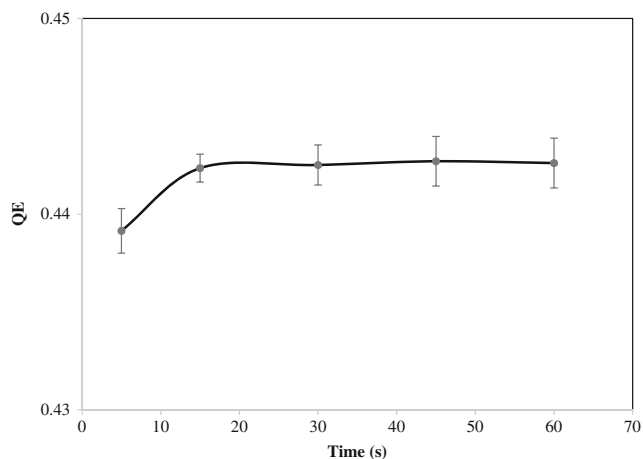


Fig. 11 Study of incubation time for quenching of QDs with 10.0 μM warfarin

TGA-CdTe QDs. From the spectra, it could be observed that TGA shows more peaks in the region of 2000.0–400.0 cm⁻¹, which are completely absent in the spectrum of TGA–CdTe. The stretching vibration of the thiol group (2550 cm⁻¹) was absent and additionally, a significant shift in the asymmetric stretching vibration of the carboxyl group (1700 cm⁻¹) was observed. As reported [37, 38], due to the formation of covalent bonds between thiol as well as carboxyls and the Cd²⁺ ions of the surface of QDs, the peaks of -SH and -COOH groups on the surface of QDs dispersed. This indicates that the thiol interacted with the surface of CdTe QDs [39].

The X-ray diffraction studies were also carried out for the powder samples of TGA-capped CdTe QDs. The powder XRD pattern is shown in Fig. 3. The three diffraction peaks of CdTe QDs at 23.74°, 39.22° and 46.12° are indexed to the (111), (220) and (311) planes of cubic CdTe lattice (JCPDS No. 15-0770). No characteristics peaks of other impurities were observed. Additionally, Scherer’s equation has been used to indicate the size of particles. The results showed a good harmony with

TEM photograph (Fig. 4) and the size of TGA-CdTe QDs was obtained as 6.5 nm. It has to be mentioned that, all XRD characterizations and calculations were performed using software “X’PERT HIGH SCORE”. TEM photograph of this TGA-CdTe QDs is shown in Fig. 4. As it can be seen, QDs were semi-spherical in shape with size distribution of 4–6 nm.

The corresponding fluorescence (FL) and UV-Vis spectra of the as-prepared TGA-CdTe QDs are shown in Fig. 5. The absorption spectrum was recorded without any dilution, while the FL spectrum were recorded for a 10.0 fold diluted solution of TGA-CdTe QDs. Corresponding fluorescence color of the synthesized QDs (Fig. 5) shows high FL intensity for TGA-CdTe QDs.

Effect of pH

The effect of different pH values on the quenching process has been investigated. Figure 6 shows the effect of pH on the quenching efficiency (QE) (Eq. 1) of QDs for 10.0 μM warfarin concentration.

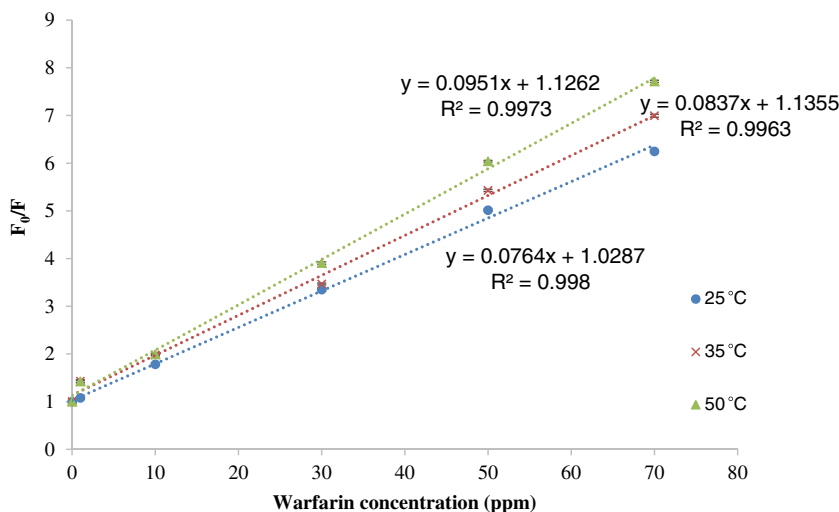
$$QE = (F_0 - F) / F_0 \tag{1}$$

Where F₀ and F represent the fluorescence intensities without and with quencher respectively. As it is shown in Fig. 6, the most suitable signals for determination of warfarin have been obtained at pH 5.0. According to pH/concentration profiles of warfarin and TGA at pH 5.0, dominant forms of warfarin is protonated while carboxyl group of TGA is deprotonated which shows that hydrogen bonding have a great role in quenching mechanism of TGA-CdTe QDs with warfarin.

Effect of Type of Buffer

To investigate the effect of buffer on the quenching process, different buffers have been prepared and then the quenching

Fig. 12 Temperature effect study



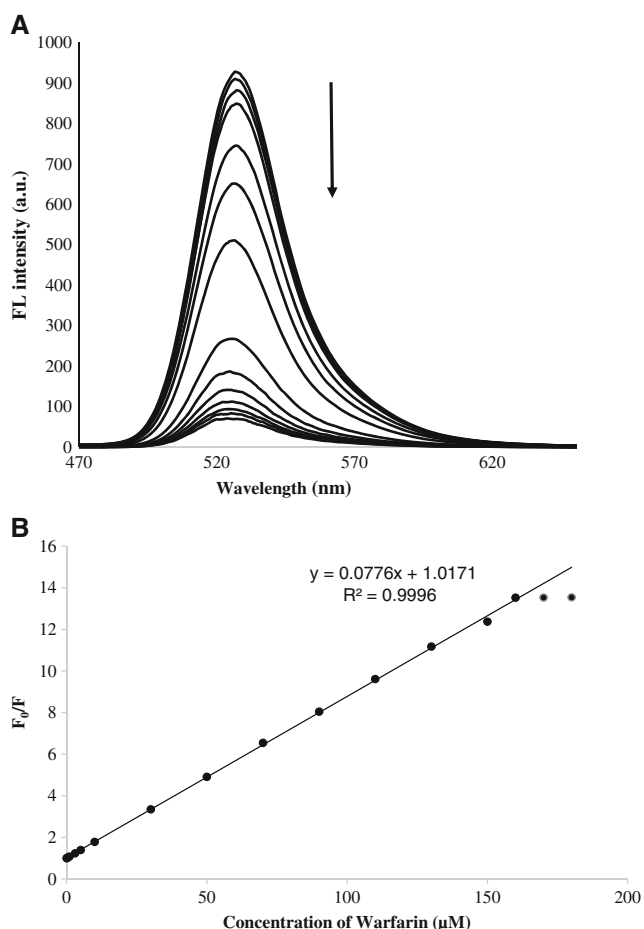


Fig. 13 a Calibration curve and b Stern-Volmer plot for determination of warfarin

of QDs fluorescence in the presence of 10.0 μM warfarin was studied. The quenching efficiency for all of the buffers has been calculated and the results are shown in Fig. 7. The best result was achieved for phosphate buffer and so, further studies were carried out in this buffer.

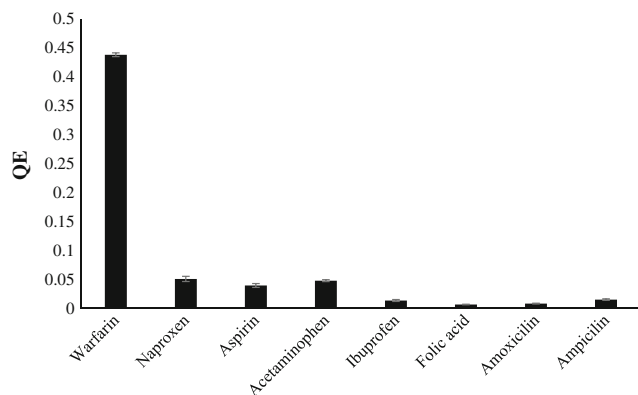


Fig. 14 Results of study of possible interferences for determination of 10.0 μM warfarin

Table 1 Determination of warfarin in real samples

Sample	Actual (μM)	Found (μM)	Recovery (%)	RSD (%) ^b
1	0.0	ND ^a	–	1.2
2	5.0	4.9	98.0	1.8
3	10.0	10.1	101.0	1.9
4	50.0	50.4	100.8	1.0
5	100.0	99.9	99.9	0.7

^a Non Detected

^b RSD determined for $n=7$

Effect of Buffer Concentration

The effect of buffer concentration was also examined. For this purpose, the quenching of FL in the presence of 10.0 μM warfarin for three different concentrations of PBS buffer was studied and the results are shown in Fig. 8. The best result was achieved for 0.01 mol L⁻¹ phosphate buffers and so, further studies were carried out in this buffer.

Effect of Ionic Strength

As shown in Fig. 8 higher concentrations of PBS cause lower quenching efficiencies. This could be the result of ionic strength enhancement. To verify this possibility, the quenching has been performed in 0.01 mol L⁻¹ phosphate buffer and different concentrations of KNO₃. As it is shown in Fig. 9, higher concentrations of KNO₃ cause the quenching efficiency to be decreased and the initial assumption for the effect of buffer concentration could be approved. To interpret this observation, the quenching mechanism must be specified. Dynamic quenching or collisional quenching occurs when the excited state fluorophore is deactivated upon contact with some other molecule (quencher) in solution [40]. In this case the fluorophore is returned to the ground state during a diffusive encounter with the quencher and the molecules are not chemically altered in the process. The Stern-Volmer equation (Eq. 2) can be used for this case:

$$F_0/F = 1 + K_{SV} \quad (2)$$

Where K_{SV} is Stern-Volmer quenching constant, which indicates the sensitivity of the fluorophore to a quencher. However, as it was mentioned, the dynamic quenching is a diffusive interaction. Therefore the ionic strength of the solution can then affect the quenching process and higher ionic strength may cause the quencher's diffusion harder and so the quenching efficiency will be lowered.

Table 2 Comparison of the present method with other reported methods for the determination of warfarin

Method	Linear range(μM)	Detection limit (μM)	Ref.
LD-DLLME HPLC–UV ^a	0.016–9.73	0.016	[43]
HPLC–FL ^b	0.003–4.9	0.0013	[44]
Electrochemistry (Stripping analysis)	0.05–0.4	0.001	[45]
Electrochemistry (MWCN/MIP ^c)	0.0001–0.002	0.00008	[46]
Cloud point extraction- FL ^d	0.003–1.0	0.33	[47]
UPLC MS/MS ^e	0.003–0.32	0.0008	[48]
Sensitized Fluorescence	5.0–500.0	2.0	[49]
Spectrophotometric method	3.2–38.9	–	[50]
Room temperature phosphorescence	16.5–79.9	7.15	[51]
DS Fluorescence spectrometry ^f	0.64–11.3	0.16	[52]
Fluorescence (TGA–CdTe QDS)	0.1–160.0	0.077	This work

^a Low-density solvent-based dispersive liquid–liquid micro-extraction-high performance liquid chromatography–ultra violet detection

^b High performance liquid chromatography with fluorescence detection

^c Multiwall carbon nanotubes and molecular imprinting

^d Cloud point extraction-fluorimetric combined methodology

^e ultra-performance liquid chromatography tandem mass spectrometry

^f Derivative synchronous fluorescence spectrometry

Effect of QDs Concentration and Incubation Time

QDs concentration has an undeniable effect on the sensitivity and linearity of determination. To study the effect of QDs concentration, different amounts of QDs stock solution were used for the quenching of 10.0 μM warfarin and the results are shown in Fig. 10. According to this data, concentration of 4.8 $\mu\text{g mL}^{-1}$ (corresponding to 60 μL QDs stock solution (100 $\mu\text{g mL}^{-1}$)) has been used for further studies. Therefore, it has to be optimized properly. High QDs concentrations may cause the spectrum to overload and lower concentrations may lead to lower sensitivity [41].

The effect of the reaction time on the fluorescence quenching of TGA–CdTe QDs by warfarin was also investigated. The results showed that the quenching occurs after about 15.0 s incubation of QDs and warfarin solution and then the fluorescence signals became stable (Fig. 11).

Effect of QDs Size

To investigate the size effect, two sizes of QDs were examined: one with the emission at 527.0 nm (synthesized under optimum conditions with 5.0 nm size) and the other with emission at 578.0 nm (larger size is expected). Equal amounts of both QDs were used to examine the quenching of warfarin. The results show that the smaller size has the higher FL intensity and the quenching efficiency is larger in this case. It is supposed that the lower FL intensity of larger QDs is due to hydrolysis of thiol

functional group of TGA which occurred at higher synthesis times and deteriorated the coating quality [42].

Mechanism of Quenching [38]

Aside from dynamic quenching, fluorescence quenching can occur by a variety of other processes. Fluorophore can form non-fluorescence complexes with quenchers. This process is referred to as static quenching since it occurs in the ground state and does not rely on diffusion or molecular collisions. To investigate the mechanism, quenching process must be performed at three different temperatures. If the temperature increase, causes the slope of calibration to be increased, the mechanism is dynamic quenching, otherwise the mechanism is static quenching. This is due to the increase in collisions at higher temperatures. The study on the quenching mechanism shows that the mechanism of quenching for warfarin is dynamic and the results are shown in Fig. 12.

Calibration Curve and Detection Limit

Under the optimum experimental conditions, the emission spectra of CdTe QDs were recorded in the presence of different amounts of warfarin. The Stern–Volmer plot of the data was linear and a linear relationship between (F_0/F) and warfarin concentration was obtained in the range of 0.1–160.0 μM with a correlation coefficient of 0.9996 (Fig. 13). The limit of detection (LOD) was calculated using $3\sigma_b/k$ equation (σ_b is the standard deviation of

blank and k is the slope of calibration curve). The LOD of the method was found to be 77.5 nM ($n=15$).

Reproducibility and Repeatability

In order to obtain reproducibility, five syntheses was performed under optimum conditions and tested for 10.0 μ M warfarin and the quenching efficiency was determined. The relative standard deviation (RSD) for 5.0 measurements was 2.11 %, revealing that this method possesses good reproducibility. The repeatability of the proposed method was attained by testing synthesized QDs for five times and the RSD was obtained as 2.36 %. Therefore, the method has a good repeatability.

Possible Interferences

The selectivity of the sensor was also tested by studying the effects of foreign species on the determination of 10.0 μ M warfarin and the results are shown in Fig. 14. The results shown are for 500.0 folds of naproxen, aspirin, and 1000.0 folds of other species. As a result, the proposed method possesses a high selectivity for warfarin.

Real Sample Analysis

Human plasma samples were selected as real samples for analysis by the developed method. Human plasma samples were centrifuged before the experiment and in order to use of the proposed method for the reality, sample required to dilute several times with phosphate buffer solution (pH 5.0). Ten tablets of warfarin were accurately weighed and ground and its solution were prepared by dissolving it in buffer and filtering the solution. Appropriate amounts of these diluted samples were spiked into the cell containing human plasma and TGA-CdTe QDs and the fluorescence intensity was recorded. As can be seen in Table 1, good recoveries and RSD were obtained revealing that the recommended method has capability in determination of warfarin plasma samples.

Conclusion

In summary, a novel method for selective determination of warfarin have been developed using TGA-capped CdTe QDs as a fluorescence probe. The advantage of this method is its simplicity, rapidity and high selectivity. The method was applied to the determination of warfarin in human plasma samples. The fluorescence quenching mechanism of warfarin interaction with TGA-CdTe QDs is presumably due to the formation of hydrogen bonds between TGA-CdTe QDs and warfarin. Table 2 shows LOD, linear range of the present method and those of other methods reported in literature for

analysis of warfarin. The results show that in some cases the present method exhibits adequately low LOD and linear response is almost better than some reported methods.

Acknowledgments We gratefully acknowledge the support of this work by Shiraz University Research Council

References

- Murray CB, Kagan C, Bawendi M (2000) Synthesis and characterization of monodisperse nanocrystals and close-packed nanocrystal assemblies. *Annu Rev Mater Sci* 30:545–610
- Sai Y, Siva Kishore N, Dattatreya A, Anand S, Sridhari G (2011) A review on biotechnology and its commercial and industrial applications. *J Biotechnol Biomater* 1:1–5
- Reed M, Randall J, Aggarwal R, Matyi R, Moore T, Wetsel A (1988) Observation of discrete electronic states in a zero-dimensional semiconductor nanostructure. *Phys Rev Lett* 60:535–537
- Gao X, Chung LW, Nie S (2007) Quantum dots for in vivo molecular and cellular imaging. In: Quantum dots. Springer pp 135–145
- Esteve-Turrillas FA, Abad-Fuentes A (2013) Applications of quantum dots as probes in immunosensing of small-sized analytes. *Biosens Bioelectron* 41:12–29
- Chakravarthy KV, Davidson BA, Helinski JD, Ding H, Law WC, Yong KT, Prasad PN, Knight PR (2011) Doxorubicin-conjugated quantum dots to target alveolar macrophages and inflammation. *Nanomed: Nanotechnol Biol Med* 7:88–96
- Adeli M, Hakimpoor F, Parsamanesh M, Kalantari M, Sobhani Z, Attyabi F (2011) Quantum dot-pseudopolyrotaxane supramolecules as anticancer drug delivery systems. *Polymer* 52: 2401–2413
- Erogbogbo F, Yong KT, Roy I, Xu G, Prasad PN, Swihart MT (2008) Biocompatible luminescent silicon quantum dots for imaging of cancer cells. *ACS Nano* 2:873–878
- Bharali DJ, Lucey DW, Jayakumar H, Pudavar HE, Prasad PN (2005) Folate-receptor-mediated delivery of InP quantum dots for bioimaging using confocal and two-photon microscopy. *J Am Chem Soc* 127:11364–11371
- Liu Z, Liu S, Wang X, Li P, He Y (2013) A novel quantum dots-based OFF-ON fluorescent biosensor for highly selective and sensitive detection of double-strand DNA. *Sens Actuators B Chem* 176:1147–1153
- Dyadyusha L, Yin H, Jaiswal S, Brown T, Baumberg J, Booy F, Melvin T (2005) Quenching of CdSe quantum dot emission, a new approach for biosensing. *Chem Commun* 25:3201–3203
- Sharma A, Pandey CM, Sumana G, Soni U, Sapra S, Srivastava A, Chatterjee T, Malhotra BD (2012) Chitosan encapsulated quantum dots platform for leukemia detection. *Biosens Bioelectron* 38:107–113
- Samia AC, Chen X, Burda C (2003) Semiconductor quantum dots for photodynamic therapy. *J Am Chem Soc* 125:15736–15737
- Jin T, Sun D, Su J, Zhang H, Sue HJ (2009) Antimicrobial efficacy of zinc oxide quantum dots against *Listeria monocytogenes*, *Salmonella enteritidis*, and *Escherichia coli* O157: H7. *J Food Sci* 74:M46–M52
- Biju V, Anas A, Akita H, Shibu ES, Itoh T, Harashima H, Ishikawa M (2012) FRET from quantum dots to photodecompose undesired acceptors and report the condensation and decondensation of plasmid DNA. *ACS Nano* 6:3776–3788
- Wang Y, Chen L (2011) Quantum dots, lighting up the research and development of nanomedicine. *Nanomed: Nanotechnol Biol Med* 7:385–402

17. Gerbec JA, Magana D, Washington A, Strouse GF (2005) Microwave-enhanced reaction rates for nanoparticle synthesis. *J Am Chem Soc* 127:15791–15800
18. Horikoshi S, Serpone N (2013). *Microwaves in nanoparticle synthesis: fundamentals and applications*. Wiley
19. Xu H, Zeiger BW, Suslick KS (2013) Sonochemical synthesis of nanomaterials. *Chem Soc Rev* 42:2555–2567
20. Kuang H, Zhao Y, Ma W, Xu L, Wang L, Xu C (2011) Recent developments in analytical applications of quantum dots. *TrAC Trends Anal Chem* 30:1620–1636
21. Gaponik N, Rogach AL (2010) Thiol-capped CdTe nanocrystals: progress and perspectives of the related research fields. *Phys Chem Chem Phys* 12:8685–8693
22. Chen D, Sharma SK, Mudhoo A (2011) *Handbook on applications of ultrasound: Sonochemistry for sustainability*. CRC press
23. Wang H, Zhu JJ, Zhu JM, Chen HY (2002) Sonochemical method for the preparation of bismuth sulfide nanorods. *J Phys Chem B* 106:3848–3854
24. Zhu JJ, Wang H, Xu S, Chen HY (2002) Sonochemical method for the preparation of monodisperse spherical and rectangular lead selenide nanoparticles. *Langmuir* 18:3306–3310
25. Zhao WB, Zhu JJ, Chen HY (2003) Photochemical preparation of rectangular PbSe and CdSe nanoparticles. *J Cryst Growth* 252:587–592
26. Qiu X, Burda C, Fu R, Pu L, Chen H, Zhu J (2004) Heterostructured Bi₂Se₃ nanowires with periodic phase boundaries. *J Am Chem Soc* 126:16276–16277
27. Kaminsky LS, Zhang ZY (1997) Human P450 metabolism of warfarin. *Pharmacol Ther* 73:67–74
28. Takahashi H, Kashima T, Kimura S, Muramoto N, Nakahata H, Kubo S, Shimoyama Y, Kajiwarra M, Echizen H (1997) Determination of unbound warfarin enantiomers in human plasma and 7-hydroxywarfarin in human urine by chiral stationary-phase liquid chromatography with ultraviolet or fluorescence and on-line circular dichroism detection. *J Chromatogr B* 701:71–80
29. Osman A, Arbring K, Lindahl TL (2005) A new high-performance liquid chromatographic method for determination of warfarin enantiomers. *J Chromatogr B* 826:75–80
30. Locatelli I, Kmetec V, Mrhar A, Grabnar I (2005) Determination of warfarin enantiomers and hydroxylated metabolites in human blood plasma by liquid chromatography with achiral and chiral separation. *J Chromatogr B* 818:191–198
31. Hou J, Zheng J, Shamsi SA (2007) Separation and determination of warfarin enantiomers in human plasma using a novel polymeric surfactant for micellar electrokinetic chromatography–mass spectrometry. *J Chromatogr A* 1159:208–216
32. Zare S (2014) M.S. Thesis, Ultrasonic- and microwave-assisted synthesis of different CdSe and CdTe quantum dots for chiral, molecular and biomolecular sensing, Shiraz University, Shiraz, Iran,
33. Zhang H, Zhou Z, Yang B, Gao M (2003) The influence of carboxyl groups on the photoluminescence of mercaptocarboxylic acid-stabilized CdTe nanoparticles. *J Phys Chem B* 107:8–13
34. Gao M, Kirstein S, Möhwald H, Rogach AL, Kornowski A, Eychmüller A, Weller H (1998) Strongly photoluminescent CdTe nanocrystals by proper surface modification. *J Phys Chem B* 102:8360–8363
35. Idowu M, Lamprecht E, Nyokong T (2008) Interaction of water-soluble thiol capped CdTe quantum dots and bovine serum albumin. *J Photochem Photobiol A Chem* 198:7–12
36. Samia A, Dayal S, Burda C (2006) Quantum dot-based energy transfer: perspectives and potential for applications in photodynamic therapy. *Ph. J Photochem Photobiol* 82:617–625
37. Li MY, Zhou HM, Zhang HY, Sun P, Yi KY, Wang M, Dong ZZ, Xu SK (2010) Preparation and purification of l-cysteine capped CdTe quantum dots and its self-recovery of degenerate fluorescence. *J Lumin* 130:1935–1940
38. Wang Y, Liu S (2012) One-pot synthesis of highly luminescent CdTe quantum dots using sodium tellurite as tellurium source in aqueous solution. *J Chil Chem Soc* 57:1109–1112
39. Jhonsi MA, Renganathan R (2010) Investigations on the photoinduced interaction of water soluble thioglycolic acid (TGA) capped CdTe quantum dots with certain porphyrins. *J Colloid Interface Sci* 344:596–602
40. Joseph RL, Lakowicz R (1999) *Principles of fluorescence spectroscopy*, vol 11. Kluwer Academic/Plenum Publishers, New York
41. Wang Q, Yu X, Zhan G, Li C (2014) Fluorescent sensor for selective determination of copper ion based on N-acetyl-l-cysteine capped CdHgSe quantum dots. *Biosens Bioelectron* 54:311–316
42. Sorouraddin MH, Imani-Nabiyi A, Najibi-Gehraz SA, Rashidi MR (2014) A new fluorimetric method for determination of valproic acid using TGA-capped CdTe quantum dots as proton sensor. *J Lumin* 145:253–258
43. Ghambari H, Hadjmohammadi MR (2012) Low-density solvent-based dispersive liquid-liquid microextraction followed by high performance liquid chromatography for determination of warfarin in human plasma. *J Chromatogr B* 899:66–71
44. Lomonac T, Ghimenti S, Piga I, Onor M, Melai B, Fuoco R, Francesco FD (2013) Determination of total and unbound warfarin and warfarin alcohols in human plasma by high performance liquid chromatography with fluorescence detection. *J Chromatogr A* 1314:54–62
45. Yau WP, Chan E (2002) Chiral CE separation of warfarin in albumin containing samples. *J Pharm Biomed Anal* 28:107–123
46. Rezaei B, Rahmanian O, Ensafi AA (2014) An electrochemical sensor based on multiwall carbon nanotubes and molecular imprinting strategy for warfarin recognition and determination. *Sens Actuators B* 196:539–545
47. Chang Z, Yan HT (2012) Cloud point extraction fluorimetric combined methodology for the determination of trace warfarin based on the sensitization effect of supramolecule. *J Lumin* 132:811–817
48. Radwan MA, Bawazeer GA, Aloudah NM, AlQuadeib BT, Aboul-Enein HY (2012) Determination of free and total warfarin concentrations in plasma using UPLC MS/MS and its application to a patient samples. *Biomed Chromatogr* 26:6–11
49. Smirnova TD, Nevryueva NV, Shtykov SN, Kochubei VI, Zhemerichkin DA (2009) Determination of warfarin by sensitized fluorescence using organized media. *J Anal Chem* 64:1114–1119
50. Sastry CSP, Rao TT, Sailaja A, Rao JV (1991) Micro-determination of warfarin sodium, nicoumalone and acebutolol hydrochloride in pharmaceutical preparations. *Talanta* 38:1107–1109
51. Pacheco ME, Bruzzone L (2014) Room temperature phosphorescence quenching study of coumarins. Indirect determination of warfarin in pharmaceuticals. *Anal Methods* 6:3462–3466
52. Panadero S, Hens G, Perez-Bendito D (1993) Simultaneous determination of warfarin and bromadiolone by derivative synchronous fluorescence spectrometry. *Talanta* 4:225–230